The US/UK

World Magnetic Model

for 2020-2025

Arnaud Chulliat
Patrick Alken
Manoj Nair
Adam Woods
Brian Meyer
Michael Paniccia (NGA)

NOAA National Centers for Environmental Information
325 Broadway
NOAA E/NE42
Boulder, CO 80305
USA

William Brown
Ciarán Beggan
Grace Cox
Susan Macmillan

British Geological Survey
Geomagnetism Team
The Lyell Centre
Research Avenue South
Edinburgh, EH14 4AP
UK

Bibliographic Reference:

Chulliat, A., W. Brown, P. Alken, C. Beggan, M. Nair, G. Cox, A. Woods, S. Macmillan, B. Meyer and M. Paniccia, 2020. *The US/UK World Magnetic Model for 2020-2025: Technical Report,* National Centers for Environmental Information, NOAA. doi: 10.25923/ytk1-yx35

ABSTRACT

This report contains a complete description of the World Magnetic Model (WMM) 2020. Section 1 contains information that users of WMM2020 require in order to implement the model and software in navigation and heading systems, and to understand magnetic charts, poles and geomagnetic coordinate systems. Section 2 contains a detailed summary of the data used and the modeling techniques employed. Section 3 contains an assessment of the model uncertainties and a description of the error model provided with the WMM2020. Section 4 contains charts of all the magnetic elements at 2020.0 and their expected annual rates of change between 2020.0 and 2025.0. These predicted changes are based upon the best knowledge of the geomagnetic main field evolution at the time the WMM was released.

Sponsored by the U.S. National Geospatial-Intelligence Agency (NGA) and the U.K. Defence Geographic Centre (DGC), the World Magnetic Model (WMM) is produced by the U.S. National Oceanic and Atmospheric Administration's National Centers for Environmental Information (NOAA/NCEI) and the British Geological Survey (BGS). It is the standard model used by the U.S. Department of Defense (DoD), the U.K. Ministry of Defence, the North Atlantic Treaty Organization (NATO) and the International Hydrographic Organization (IHO), for navigation, attitude and heading referencing systems using the geomagnetic field. It is also used widely in civilian navigation and heading systems.

The WMM2020 product release includes several software items by which the WMM2020 model may be computed and/or its subroutines incorporated into larger DoD systems. It is hoped that the software provided is useful for most occasions of DoD systems procurement and development.

CONTACTS

The model, associated software, digital charts and documentation are available at https://www.ngdc.noaa.gov/geomag/WMM/ or by contacting NCEI, BGS, or NGA.

Please cite using these identifiers. Recommended usage and additional information available at:

Technical Report – doi: 10.25923/ytk1-yx35

Dataset – doi: 10.25921/11v3-da71

MODEL AND SOFTWARE SUPPORT

National Centers for Environmental Information

NOAA E/NE42
325 Broadway
Boulder, CO 80305
USA
Attention: Manoj Nair or Arnaud Chulliat
Phone: + (303) 497-4642 or -6522
Email: geomag.models@noaa.gov
Web: https://www.ngdc.noaa.gov/geomag/WMM/

British Geological Survey

The Lyell Centre
Research Avenue South
Edinburgh, EH14 4AP
UK
Attention: Susan Macmillan or William Brown
Phone: + 44 131 667 1000
Email: smac@bgs.ac.uk or wb@bgs.ac.uk
Web: https://geomag.bgs.ac.uk/research/modelling/WorldMagneticModel.html

APPLICABILITY WITHIN THE U.S. DEPARTMENT OF DEFENSE

National Geospatial-Intelligence Agency

Geomatics Office
NGA-SN, Mail Stop L-41
3838 Vogel Road
Arnold, MO 63010-6238
U.S.A.

Email: WGS84@nga.mil

APPLICABILITY WITHIN THE U.K. MINISTRY OF DEFENCE

Defence Geographic Centre

MacLeod Building, Elmwood Avenue
Feltham
Middlesex, TW13 7AH
UK

Chris Mundy
Email: Chris.Mundy601@mod.gov.uk

Matthew Shimell
Email: Matthew.Shimell113@mod.gov.uk

Giles André
Email: Giles.Andre562@mod.gov.uk

The NATO and military specifications for magnetic models are STANAG 7172 (NATO Standardization Agency, 2011) and MIL-PRF-89500B (Department of Defense, 2019). Magnetic model requirements that are more stringent than those set forth in these specifications should be addressed to NCEI and BGS (e.g., those that must include magnetic effects of the Earth's crust, ionosphere, or magnetosphere and/or require greater spatial or temporal resolution on a regional or local basis).

ACKNOWLEDGEMENTS

This work was carried out under the sponsorship of the U.S. National Geospatial-Intelligence Agency (NGA) and the UK Ministry of Defence, Defence Geographic Centre (DGC). The maps of the geomagnetic elements were designed by Jesse Varner (NOAA/NCEI and Cooperative Institute for Research in the Environmental Sciences, University of Colorado Boulder). Thank you to Barbara Ambrose in the NCEI Communications team for helping with the formatting and for making sure this document is accessible by people with disabilities. Eric Kihn (NOAA/NCEI) is the U.S. manager for the WMM project, which is funded by NGA. NGA personnel oversee the WMM development, reviewed this report and contributed to the error analysis. Data from the Swarm satellite mission were provided by the European Space Agency (ESA), supported by ESA member states. Many institutes and agencies are involved in the operation of geomagnetic observatories around the world. In particular we would like to thank: Centre de Recherche en Astronomie Astrophysique et Geophysique, ALGERIA; Servicio Meteorologico Nacional, ARGENTINA; Universidad Nacional de la Plata, ARGENTINA; Geoscience Australia, AUSTRALIA; Zentralanstalt für Meteorologie und Geodynamik, AUSTRIA; Institut Royal Météorologique de Belgique, BELGIUM; CNPq-Observatório Nacional, BRAZIL; Academy of Sciences,

BULGARIA; Natural Resources Canada, CANADA; Centro Meteorológico Regional Pacifico, CHILE; Academy of Sciences, CHINA; China Earthquake Administration, CHINA; Instituto Geográfico Agustín Codazzi, COLOMBIA; University of Zagreb, CROATIA; Academy of Sciences, CZECH REPUBLIC; Danish Technical University, DENMARK; Addis Ababa University, ETHIOPIA; Finnish Meteorological Institute, FINLAND; Sodankylä Geophysical Observatory, FINLAND; Institut de Physique du Globe de Paris, FRANCE; Ecole et Observatoire des Sciences de la Terre, FRANCE; Ludwig Maximilians University Munich, GERMANY; Alfred-Wegener-Institute for Polar & Marine Research, GERMANY; Helmholtz Centre Potsdam, GERMANY; Universities of Karlsruhe and Stuttgart, GERMANY; Institute of Geology and Mineral Exploration, GREECE; Academy of Sciences, HUNGARY; Eötvös Loránd Geophysical Institute of Hungary, HUNGARY; University of Iceland, ICELAND; Indian Institute of Geomagnetism, INDIA; National Geophysical Research Institute, INDIA; Meteorological and Geophysical Agency, INDONESIA; The Irish Meteorological Service, IRELAND; Survey of Israel, ISRAEL; Instituto Nazionale di Geofisica e Vulcanologia, ITALY; Japan Coast Guard, JAPAN; Japan Meteorological Agency, JAPAN; Geographical Survey Institute, JAPAN; Institute of the Ionosphere, KAZAKHSTAN; Korean Meteorological Administration, KOREA; National Centre for Geophysical Research, LEBANON; Université d'Antananarivo, MADAGASCAR; Gan Meteorological Office, MALDIVES; Institute of Geological and Nuclear Sciences, NEW ZEALAND; University of Tromsø, NORWAY; Instituto Geofísico del Perú, PERU; Academy of Sciences, POLAND; Instituto Nacional de Geologia, REPÚBLICA DE MOÇAMBIQUE; Geological Survey of Romania, ROMANIA; Academy of Sciences, RUSSIA; Institute of Solar-Terrestrial Physics, RUSSIA; Dept. of Agriculture, Forestry, Fisheries & Meteorology, SAMOA; Geomagnetic College Grocka, SERBIA & MONTENEGRO; Slovenska Akademia Vied, SLOVAKIA; National Research Foundation, SOUTH AFRICA; Observatori de l'Ebre, SPAIN; Real Instituto y Observatorio de la Armada, SPAIN; Instituto Geográfico Nacional, SPAIN; Sveriges Geologiska Undersökning, SWEDEN; Swedish Institute of Space Physics, SWEDEN; ETH Zurich, SWITZERLAND; Earthquake Research Institute, TURKEY; US Geological Survey, UNITED STATES OF AMERICA; British Geological Survey, UNITED KINGDOM; Academy of Sciences, UKRAINE; Ukrainian Antarctic Center, UKRAINE and National Centre for Science and Technology, VIETNAM. The INTERMAGNET program and ICSU World Data System (primarily the World Data Centre for Geomagnetism, Edinburgh) assist in the quality control and dissemination of observatory data. The magnetic activity indices Kp and Dst were computed and provided by Helmholtz Centre Potsdam (GFZ), Germany and World Data Center for Geomagnetism in Kyoto, respectively. We acknowledge use of NASA/GSFC's Space Physics Data Facility's ftp service, and OMNI data, particularly measurements from the NASA/ACE and NOAA/DSCOVR missions. This model could not have been produced without the efforts of all of these institutes.

TABLE OF CONTENTS

1. THE MODEL

1.1 INTRODUCTION

The Earth is like a giant magnet. At every location on or above the Earth, its magnetic field has a more or less well-known direction, which can be used to orient ships, aircraft, satellites, antennas, drilling equipment and handheld devices. At some places on the globe the horizontal direction of the magnetic field coincides with the direction of geographic north ("true" north), but in general this is not the case. The angular amount by which the horizontal direction of the magnetic field differs from true north is called the magnetic declination, or simply declination (D, see Figure 1). This is the correction required to convert between a magnetic bearing and a true bearing. The main utility of the World Magnetic Model (WMM) is to provide magnetic declination for any desired location on the globe. In addition to the magnetic declination, the WMM also provides the complete geometry of the field from 1 km below the World Geodetic System (WGS 84) ellipsoid surface to approximately 850 km above it (MIL-PRF-89500B, Department of Defense, 2019). The magnetic field extends deep into the Earth and far out into space, but the WMM is not valid at these extremes.

The Earth's magnetism has several sources. All sources affect a scientific or navigational instrument but only some are represented in the WMM. The strongest contribution, by far, is the magnetic field produced by the Earth's liquid-iron outer core, called the "core field". Magnetic minerals in the crust and upper mantle make a further contribution that can be locally significant. Electric currents induced by the flow of conducting sea water through the ambient magnetic field make a further, albeit weak, contribution to the observed magnetic field. All of these are of "internal" origin and their large-scale components (see below) are included in the WMM. Deliberately excluded from the WMM by the data selection process and by other means (e.g., model co-estimation) are so-called "disturbance fields". These are contributions arising from electric currents in the upper atmosphere and near-Earth space. These "external" magnetic fields are time-varying, and have a further effect. They induce electric currents in the Earth and oceans, producing secondary internal magnetic fields, which are considered part of the disturbance field and are not represented in the WMM.

The mathematical representation of the WMM is an expansion of the magnetic potential into spherical harmonic functions to degree and order 12. The minimum wavelength resolved is 360° / $\sqrt{12 \times 13}$ = 28.8° in arc-length, corresponding to 3200 km at the Earth's surface (see section 3.6.3 of Backus et al., 1996). The WMM is a model of those internal magnetic fields that are not part of the disturbance field and have spatial wavelengths exceeding 30° in arc-length. This works out to be almost the entire core field and the long-wavelength portion of the crustal and oceanic fields. In this report, the term "main field" refers to the portion of the Earth's magnetic field at epoch 2020.0 that is modeled by the WMM.

The core field changes perceptibly from year to year. This effect, called secular variation (SV), is accounted for in the WMM by a linear SV model. Specifically, a straight line is used as the model of the time-dependence of each coefficient of the spherical harmonic representation of the magnetic potential (see section 1.2). Due to unpredictable non-linear changes in the core field, the values of the WMM coefficients have to be updated every five years. The revision described in this report, WMM2020, is valid from 2020.0 to 2025.0.

1.1.1 MAGNETIC ELEMENTS

The geomagnetic field vector, $\mathbf{B}_m$, is described by seven elements. These are the northerly intensity *X*, the easterly intensity *Y*, the vertical intensity *Z* (positive downwards) and the following quantities derived from *X*, *Y* and *Z*: the horizontal intensity *H*, the total intensity *F*, the inclination angle *I*, (also called the dip angle and measured from the horizontal plane to the field vector, positive downwards) and the declination angle *D* (also called the magnetic variation and measured clockwise from true north to the horizontal component of the field vector). In the descriptions of *X, Y, Z, H, F, I* and *D* above, the vertical direction is perpendicular to the WGS 84 ellipsoid model of the Earth, the horizontal plane is perpendicular to the vertical direction, and the rotational directions clockwise and counter-clockwise are determined by a view from above (see Figure 1).

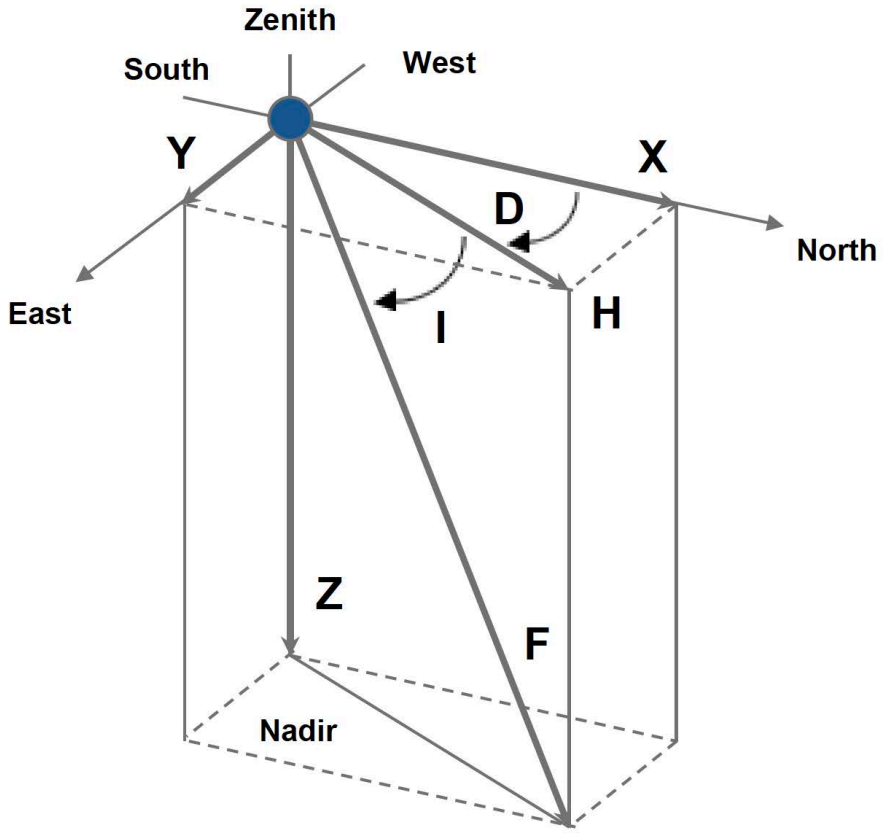

Figure 1: The seven elements of the geomagnetic field vector B_m associated with an arbitrary point in space.

The quantities *X, Y* and *Z* are the sizes of perpendicular vectors that add vectorially to $\mathbf{B}_m$. Conversely, *X*, *Y* and *Z* can be determined from the quantities *F*, *I* and *D* (i.e., the quantities that specify the size and direction of $\mathbf{B}_m$).

1.1.2 GRID VARIATION

In the polar regions, or near the rotation axis of the Earth, the angle *D* changes strongly with a change in the longitude of the observer, and is therefore a poor measure of the direction of $\mathbf{B}_m$. For this reason, the WMM specification (MIL-PRF-89500B, Department of Defense, 2019) defines two

auxiliary angles, called grid variation north (GV_N) and south (GV_S), for the direction of $\mathbf{B}_m$ in the horizontal plane in each polar region. Their definitions are:

$$\begin{aligned} GV_N &= D - \lambda \quad \text{for } \varphi > 55° \\ GV_S &= D + \lambda \quad \text{for } \varphi < -55° \end{aligned} \tag{1}$$

where λ is the longitude and φ is the geodetic latitude.

The quantities GV_N and GV_S defined above are examples of a more general concept, namely grid variation (also called grid magnetic angle or grivation). At a location on the plane of a chosen horizontal grid coordinate system, grivation is the angle between grid north and magnetic north, i.e., the angle measured clockwise from the direction parallel to the grid's Northing axis to the horizontal component of the magnetic field at the observer's location. Grivation is useful for local surveys, where location is given by grid coordinates rather than by longitude and latitude. It is dependent on the map projection used to define the grid coordinates. In general, it is

$$GV_{grid} = D - C \tag{2}$$

where D is the magnetic declination and C is the "convergence-of-meridians" defined as the clockwise angle from the northward meridional arc to the grid Northing direction.

For example, large scale military topographic mapping routinely employs the Universal Transverse Mercator (UTM) grid coordinates for the map projection of the sheet, for the definition of a grid to overprint, and for a grivation calculation as defined above. Above 84°N and below 80°S, it employs the Universal Polar Stereographic (UPS) grid. For these two grids, the grid variation could be notated GV_{UTM} and GV_{UPS}, respectively.

In the WMM subroutine library, both GV_{UPS} and GV_{UTM} are provided within certain restrictions (see the software user's guide, https://www.ngdc.noaa.gov/geomag/WMM/soft.shtml).

1.1.3 RANGE OF THE MAGNETIC ELEMENTS AT THE EARTH'S SURFACE

Table 1 shows the expected range of the magnetic field elements and *GV* at the Earth's surface.

Table 1: Ranges of magnetic elements and *GV* at the Earth's surface.

Element	Name	Alternative Name	Range at Earth's Surface			
X	North component	Northerly intensity	-17000	43000	nT	North
Y	East component	Easterly intensity	-18000	17000	nT	East
Z	Down component	Vertical intensity	-67000	62000	nT	Down
H	Horizontal intensity		0	43000	nT	
F	Total intensity	Total field	23000	67000	nT	
I	Inclination	Dip	-90	90	Degree	Down
D	Declination	Magnetic variation	-180	180	Degree	East / Clockwise
GV	Grid variation	Grivation	-180	180	Degree	East / Clockwise

1.2 RELEVANT MODEL EQUATIONS

This section describes the representation of the magnetic field in the WMM and lists the equations needed to obtain the magnetic field elements for the desired location and time from the WMM coefficients. All variables in this section adhere to the following measurement conventions: angles are in radians, lengths are in meters, magnetic intensities are in nanoteslas (nT, where one tesla is one weber per square meter or one $kg.s^{-2}.A^{-1}$) and times are in years. The software may display these quantities in other units, which it will identify.

The main magnetic field $\mathbf{B}_m$ is a potential field and therefore can be written in geocentric spherical coordinates (longitude λ, latitude φ', radius r) as the negative spatial gradient of a scalar potential

$$\mathbf{B}_m(\lambda, \varphi', r, t) = -\nabla V(\lambda, \varphi', r, t) \tag{3}$$

where t is the time. This potential can be expanded in terms of spherical harmonics:

$$V(\lambda, \varphi', r, t) = a \sum_{n=1}^{N} \left(\frac{a}{r}\right)^{n+1} \sum_{m=0}^{n} (g_n^m(t) \cos(m\lambda) + h_n^m(t) \sin(m\lambda)) \breve{P}_n^m(\sin \varphi') \tag{4}$$

where *N*=12 is the degree of the expansion of the WMM, a (6371200 m) is the geomagnetic reference radius (which is close to the mean Earth radius), (λ, φ', r) are the longitude, latitude and radius in a spherical geocentric reference frame, and $g_n^m(t)$ and $h_n^m(t)$ are the time-dependent Gauss coefficients of degree *n* and order *m* describing the Earth's main magnetic field. For any real number μ, $\breve{P}_n^m(\mu)$ are the Schmidt semi-normalized associated Legendre functions defined as:

$$\begin{aligned} \breve{P}_n^m(\mu) &= \sqrt{2\frac{(n-m)!}{(n+m)!}}\, P_{n,m}(\mu) \;\; if \;\; m > 0 \\ \breve{P}_n^m(\mu) &= \qquad\qquad P_{n,m}(\mu) \;\; if \;\; m = 0 \end{aligned} \tag{5}$$

Here, the definition of $P_{n,m}(\mu)$ is commonly used in geodesy and geomagnetism (e.g., Heiskanen and Moritz, 1967, equation 1-60; Langel, 1987, equation 8). Sample functions, for geocentric latitude φ', are:

$$
\begin{aligned}
P_{3,0}(\sin\varphi') &= \frac{1}{2}(\sin\varphi')(5\sin^2\varphi'-3) \\
P_{3,1}(\sin\varphi') &= -\frac{3}{2}(\cos\varphi')(1-5\sin^2\varphi') \\
P_{3,2}(\sin\varphi') &= 15(\sin\varphi')(1-\sin^2\varphi') \\
P_{3,3}(\sin\varphi') &= 15\cos^3\varphi'
\end{aligned}
\tag{6}
$$

These $P_{n,m}(\mu)$ are related to the $P_n^m(\mu)$ defined in Abramowitz and Stegun (1972, Chapter 8) or Gradshteyn and Ryzhik (1994, Chapter 8.7) by $P_{n,m}(\mu) = (-1)^m P_n^m(\mu)$.

WMM2020 comprises two sets of Gauss coefficients to degree and order *N=12*. One set provides a spherical harmonic main field model for 2020.0 in units of nT, the other set provides a predictive secular variation model for the period 2020.0 to 2025.0 in units of nT/year. The secular variation model was derived from geomagnetic data prior to 2020.0. Specifically, it is the average of two models: one representing the average change of the main field over a year starting at 2018.5; the other representing the extrapolated change of the main field in 2020.0. However, this represents our best knowledge of the geomagnetic main field evolution at the time of the WMM release, and is expected to yield geomagnetic main field values within defined uncertainty parameters for the lifetime of the model.

A step by step procedure is provided below for computing the magnetic field elements at a given location and time (λ, φ, h_{MSL}, t), where λ and φ are the longitude and geodetic latitude, h_{MSL} is height above Mean Sea Level (MSL), and t is the time given in decimal years.

In the first step, the user provides the time, location and height above MSL at which the magnetic elements are to be calculated. The height above MSL is then converted to height *h* above the WGS 84 ellipsoid by using the geopotential model EGM96 (Lemoine et al., 1998). This is accomplished by interpolating a grid of the geoid height file with a spatial resolution of 15 arc-minutes. This stage of converting height above MSL to height above the WGS 84 ellipsoid has a very small effect on the resulting magnetic field values (of the order of 1 nT or less) and is unnecessary in the majority of implementations. Note that the user can also directly enter the height above the WGS 84 ellipsoid into the software.

The geodetic coordinates (*λ, φ, h)* are then transformed into spherical geocentric coordinates (*λ, φ´, r*) by recognizing that *λ* is the same in both coordinate systems, and that (*φ´, r*) is computed from (*φ, h*) according to the equations:

$$\begin{aligned} p &= (R_c + h)\cos\varphi \\ z &= (R_c(1-e^2) + h)\sin\varphi \\ r &= \sqrt{p^2 + z^2} \\ \varphi' &= \arcsin\frac{z}{r} \end{aligned} \tag{7}$$

Here, $p = \sqrt{x^2 + y^2}$, where *x*, *y* and *z* are the coordinates of a geocentric Cartesian coordinate system in which the positive *x* and *z* axes point in the directions of the prime meridian (*λ=0*) and the Earth's rotation axis, respectively. The semi-major axis *A,* reciprocal flattening *1/f,* eccentricity squared e^2 and radius of curvature of the prime vertical (also called normal section) R_c at the given latitude *φ* are given for the WGS 84 ellipsoid as

$$\begin{aligned} A &= 6378137\ m \\ \frac{1}{f} &= 298.257223563 \\ e^2 &= f(2-f) \end{aligned} \tag{8}$$

$$R_c = \frac{A}{\sqrt{1 - e^2 \sin^2 \varphi}}$$

In the second step, the Gauss coefficients $g_n^m(t)$ and $h_n^m(t)$ are determined for the desired time *t* from the model coefficients $g_n^m(t_0)$, $h_n^m(t_0)$, $\dot{g}_n^m(t_0)$ and $\dot{h}_n^m(t_0)$ as

$$\begin{aligned} g_n^m(t) &= g_n^m(t_0) + (t - t_0)\,\dot{g}_n^m(t_0) \\ h_n^m(t) &= h_n^m(t_0) + (t - t_0)\,\dot{h}_n^m(t_0) \end{aligned} \tag{9}$$

where the time is given in decimal years and $t_0 = 2020.0$, the reference epoch of the model. The quantities $g_n^m(t_0)$ and $h_n^m(t_0)$ are called the main field coefficients and the quantities $\dot{g}_n^m(t_0)$ and $\dot{h}_n^m(t_0)$ are called the secular variation coefficients.

In the third step, the field vector components *X′*, *Y′* and *Z′* in geocentric coordinates are computed as

$$\begin{aligned} X'(\lambda, \varphi', r) &= -\frac{1}{r}\frac{\partial V}{\partial \varphi'} \\ &= -\sum_{n=1}^{12}\left(\frac{a}{r}\right)^{n+2} \sum_{m=0}^{n} (g_n^m(t)\cos m\lambda + h_n^m(t)\sin m\lambda)\frac{d\,\breve{\mathrm{P}}_n^m(\sin\varphi')}{d\varphi'} \end{aligned} \tag{10}$$

$$\begin{aligned} Y'(\lambda, \varphi', r) &= -\frac{1}{r\cos\varphi'}\frac{\partial V}{\partial \lambda} \\ &= \frac{1}{\cos\varphi'}\sum_{n=1}^{12}\left(\frac{a}{r}\right)^{n+2} \sum_{m=0}^{n} m(g_n^m(t)\sin m\lambda - h_n^m(t)\cos m\lambda)\,\breve{\mathrm{P}}_n^m(\sin\varphi') \end{aligned} \tag{11}$$

$$
\begin{aligned}
Z'(\lambda,\varphi',r) &= \frac{\partial V}{\partial r} \\
&= -\sum_{n=1}^{12}(n+1)\left(\frac{a}{r}\right)^{n+2}\sum_{m=0}^{n}(g_n^m(t)\cos m\lambda + h_n^m(t)\sin m\lambda)\breve{\mathrm{P}}_n^m(\sin\varphi')
\end{aligned}
\tag{12}
$$

At this point, the secular variation of the field components can be computed as

$$
\begin{aligned}
\dot{X}'(\lambda,\varphi',r) &= -\frac{1}{r}\frac{\partial \dot{V}}{\partial \varphi'} \\
&= -\sum_{n=1}^{12}\left(\frac{a}{r}\right)^{n+2}\sum_{m=0}^{n}(\dot{g}_n^m\cos m\lambda + \dot{h}_n^m\sin m\lambda)\frac{d\breve{\mathrm{P}}_n^m(\sin\varphi')}{d\varphi'}
\end{aligned}
\tag{13}
$$

$$
\begin{aligned}
\dot{Y}'(\lambda,\varphi',r) &= -\frac{1}{r\cos\varphi'}\frac{\partial \dot{V}}{\partial \lambda} \\
&= \frac{1}{\cos\varphi'}\sum_{n=1}^{12}\left(\frac{a}{r}\right)^{n+2}\sum_{m=0}^{n}m(\dot{g}_n^m\sin m\lambda - \dot{h}_n^m\cos m\lambda)\breve{\mathrm{P}}_n^m(\sin\varphi')
\end{aligned}
\tag{14}
$$

$$
\begin{aligned}
\dot{Z}'(\lambda,\varphi',r) &= \frac{\partial \dot{V}}{\partial r} \\
&= -\sum_{n=1}^{12}(n+1)\left(\frac{a}{r}\right)^{n+2}\sum_{m=0}^{n}(\dot{g}_n^m\cos m\lambda + \dot{h}_n^m\sin m\lambda)\breve{\mathrm{P}}_n^m(\sin\varphi')
\end{aligned}
\tag{15}
$$

$$
\frac{d\breve{\mathrm{P}}_n^m(\sin\varphi')}{d\varphi'} = (n+1)(\tan\varphi')\breve{\mathrm{P}}_n^m(\sin\varphi') - \sqrt{(n+1)^2 - m^2}\,(\sec\varphi')\breve{\mathrm{P}}_{n+1}^m(\sin\varphi') \tag{16}
$$

In the fourth step, the geocentric magnetic field vector components *X′*, *Y′* and *Z′*, are rotated into the ellipsoidal reference frame, using

$$
\begin{aligned}
X &= X'\cos(\varphi' - \varphi) - Z'\sin(\varphi' - \varphi) \\
Y &= Y' \\
Z &= X'\sin(\varphi' - \varphi) + Z'\cos(\varphi' - \varphi)
\end{aligned}
\tag{17}
$$

Similarly, the time derivatives of the vector components, $\dot{X}'$, $\dot{Y}'$ and $\dot{Z}'$ are rotated using

$$
\begin{aligned}
\dot{X} &= \dot{X}'\cos(\varphi' - \varphi) - \dot{Z}'\sin(\varphi' - \varphi) \\
\dot{Y} &= \dot{Y}' \\
\dot{Z} &= \dot{X}'\sin(\varphi' - \varphi) + \dot{Z}'\cos(\varphi' - \varphi)
\end{aligned}
\tag{18}
$$

In the last step, the magnetic elements *H, F, I* and *D* are computed from the orthogonal components:

$$
H = \sqrt{X^2 + Y^2}, \quad F = \sqrt{H^2 + Z^2}, \quad I = \arctan(Z, H), \quad D = \arctan(Y, X) \tag{19}
$$

where $\arctan(a, b)$ is $\tan^{-1}(a/b)$, taking into account the angular quadrant, avoiding a division by zero, and resulting in a declination in the range of *-π* to *π* and an inclination in the range of *-π/2* to *π/2*. These angles in radians are then output by the WMM software in degrees.

The secular variation of these elements is computed using

$$
\begin{aligned}
\dot{H} &= \frac{X \cdot \dot{X} + Y \cdot \dot{Y}}{H} \\
\dot{F} &= \frac{X \cdot \dot{X} + Y \cdot \dot{Y} + Z \cdot \dot{Z}}{F} \\
\dot{I} &= \frac{H \cdot \dot{Z} - Z \cdot \dot{H}}{F^2} \\
\dot{D} &= \frac{X \cdot \dot{Y} - Y \cdot \dot{X}}{H^2} \\
G\dot{V} &= \dot{D}
\end{aligned}
\tag{20}
$$

where $\dot{I}$, $\dot{D}$ and $\dot{GV}$ are given in radians per year. The WMM software then outputs these angles in arc-minutes per year or decimal degrees per year.

1.3 THE WMM2020 COEFFICIENTS

The model coefficients, also referred to as Gauss coefficients, are listed in Table 2. These coefficients can be used to compute values for the field elements and their annual rates of change at any location near the surface of the Earth, and at any date between 2020.0 and 2025.0.

Table 2: Final coefficients for WMM2020. Units are nT for the main field, and nT per year for the secular variation. The index *n* is the degree and *m* is the order. Since $h_n^m(t_0)$ and $\dot{h}_n^m(t_0)$ are not defined for $m = 0$, the corresponding fields are left blank. (The corresponding coefficients are set to zero in the WMM2020 coefficient file.)

n	m	$g_n^m(t_0)$	$h_n^m(t_0)$	$\dot{g}_n^m(t_0)$	$\dot{h}_n^m(t_0)$
1	0	-29404.5		6.7	
1	1	-1450.7	4652.9	7.7	-25.1
2	0	-2500.0		-11.5	
2	1	2982.0	-2991.6	-7.1	-30.2
2	2	1676.8	-734.8	-2.2	-23.9
3	0	1363.9		2.8	
3	1	-2381.0	-82.2	-6.2	5.7
3	2	1236.2	241.8	3.4	-1.0
3	3	525.7	-542.9	-12.2	1.1
4	0	903.1		-1.1	
4	1	809.4	282.0	-1.6	0.2
4	2	86.2	-158.4	-6.0	6.9
4	3	-309.4	199.8	5.4	3.7
4	4	47.9	-350.1	-5.5	-5.6
5	0	-234.4		-0.3	
5	1	363.1	47.7	0.6	0.1
5	2	187.8	208.4	-0.7	2.5
5	3	-140.7	-121.3	0.1	-0.9
5	4	-151.2	32.2	1.2	3.0
5	5	13.7	99.1	1.0	0.5
6	0	65.9		-0.6	
6	1	65.6	-19.1	-0.4	0.1
6	2	73.0	25.0	0.5	-1.8
6	3	-121.5	52.7	1.4	-1.4
6	4	-36.2	-64.4	-1.4	0.9
6	5	13.5	9.0	0.0	0.1
6	6	-64.7	68.1	0.8	1.0
7	0	80.6		-0.1	
7	1	-76.8	-51.4	-0.3	0.5
7	2	-8.3	-16.8	-0.1	0.6
7	3	56.5	2.3	0.7	-0.7
7	4	15.8	23.5	0.2	-0.2
7	5	6.4	-2.2	-0.5	-1.2
7	6	-7.2	-27.2	-0.8	0.2
7	7	9.8	-1.9	1.0	0.3
8	0	23.6		-0.1	
8	1	9.8	8.4	0.1	-0.3
8	2	-17.5	-15.3	-0.1	0.7
8	3	-0.4	12.8	0.5	-0.2
8	4	-21.1	-11.8	-0.1	0.5
8	5	15.3	14.9	0.4	-0.3
8	6	13.7	3.6	0.5	-0.5
8	7	-16.5	-6.9	0.0	0.4
8	8	-0.3	2.8	0.4	0.1
9	0	5.0		-0.1	
9	1	8.2	-23.3	-0.2	-0.3
9	2	2.9	11.1	0.0	0.2
9	3	-1.4	9.8	0.4	-0.4
9	4	-1.1	-5.1	-0.3	0.4
9	5	-13.3	-6.2	0.0	0.1
9	6	1.1	7.8	0.3	0.0
9	7	8.9	0.4	0.0	-0.2
9	8	-9.3	-1.5	0.0	0.5
9	9	-11.9	9.7	-0.4	0.2
10	0	-1.9		0.0	
10	1	-6.2	3.4	0.0	0.0
10	2	-0.1	-0.2	0.0	0.1
10	3	1.7	3.5	0.2	-0.3
10	4	-0.9	4.8	-0.1	0.1
10	5	0.6	-8.6	-0.2	-0.2
10	6	-0.9	-0.1	0.0	0.1
10	7	1.9	-4.2	-0.1	0.0
10	8	1.4	-3.4	-0.2	-0.1
10	9	-2.4	-0.1	-0.1	0.2
10	10	-3.9	-8.8	0.0	0.0
11	0	3.0		0.0	
11	1	-1.4	0.0	-0.1	0.0
11	2	-2.5	2.6	0.0	0.1
11	3	2.4	-0.5	0.0	0.0
11	4	-0.9	-0.4	0.0	0.2
11	5	0.3	0.6	-0.1	0.0
11	6	-0.7	-0.2	0.0	0.0
11	7	-0.1	-1.7	0.0	0.1
11	8	1.4	-1.6	-0.1	0.0
11	9	-0.6	-3.0	-0.1	-0.1
11	10	0.2	-2.0	-0.1	0.0
11	11	3.1	-2.6	-0.1	0.0
12	0	-2.0		0.0	
12	1	-0.1	-1.2	0.0	0.0
12	2	0.5	0.5	0.0	0.0
12	3	1.3	1.3	0.0	-0.1
12	4	-1.2	-1.8	0.0	0.1
12	5	0.7	0.1	0.0	0.0
12	6	0.3	0.7	0.0	0.0
12	7	0.5	-0.1	0.0	0.0
12	8	-0.2	0.6	0.0	0.1
12	9	-0.5	0.2	0.0	0.0
12	10	0.1	-0.9	0.0	0.0
12	11	-1.1	0.0	0.0	0.0
12	12	-0.3	0.5	-0.1	-0.1

1.4 SINGULARITIES AT THE GEOGRAPHIC POLES

The World Magnetic Model has singularities at the North and South geographic poles. This is a mathematical issue, not a geophysical phenomenon, stemming from the ambiguity of longitude at a Pole and at any altitude over a Pole. Related to this, the North-East-Down (NED) frame of unit vectors to which the *X′*, *Y′*, *Z′* quantities are referred is defined everywhere except at or over a Pole. This section extends these concepts. The North Pole is discussed in the following, with similar implications for the South Pole.

To most comprehensively appreciate the model equations, let the arbitrariness of the North Pole's longitude disambiguate the North Pole's NED frame. In other words, if the Pole is assigned a longitude of λ, then the NED frame at the Pole is to be oriented so that the unit vector "N" of NED has the same direction as for a point approaching the pole along the λ-meridian, the unit vector "D" is directed downward, and the unit vector "E" is directed so that NED is right-handed. This is equivalent to requiring the NED frame at longitude λ and latitude 90° to be the limit of NED frames as the latitude approaches 90° and the longitude and altitude remain fixed.

On 1 January 2020, directly above the North (resp. South) Pole at 6,371,200 meters from the Earth's center, the magnetic field vector lies in the half-plane of the 176.68°W (resp. 30.83°W) meridian. If the Pole is assigned $\lambda = 0°$, the components *X′*, *Y′*, *Z′* (also the components *X*, *Y*, *Z*) are 1797.7 nT, 104.3 nT, and 56386.7 nT respectively at the North Pole, 14276.5 nT, -8520.4 nT and -51671.3 nT respectively at the South Pole. A change in the longitude assigned to the Pole is equivalent to a rotation of the NED frame about the polar axis.

The model equations of section 1.2 support the above pole calculation and others like it provided the equation for *Y′* is extended by continuity as follows to ameliorate the factor $\cos(\varphi')$ in the denominator. As φ' approaches 90°, the function $(\check{P}_n^m(\sin\varphi'))/\cos\varphi'$ approaches zero if $m > 1$. It approaches certain non-zero finite limits if $m = 1$. It multiplies a zero coefficient and can be ignored if $m = 0$. For $m = 1$ and $1 \le n \le 12$ respectively, the limits are:

1	2	3	4	5	6	7	8	9	10	11	12
1	$\sqrt{3}$	$\sqrt{6}$	$\sqrt{10}$	$\sqrt{15}$	$\sqrt{21}$	$2\sqrt{7}$	6	$3\sqrt{5}$	$\sqrt{55}$	$\sqrt{66}$	$\sqrt{78}$

1.5 MODEL EQUATIONS NUMERICAL EXAMPLE

A software implementation of the relevant model equations is provided with this report. Most software developers should find the C programs and/or C subroutines to be sufficient for their purposes, after adaptations are made to their own software structures.

To aid software developers who need to re-implement the model equations for special requirements, Tables 3a to 3c provide a numerical example showing the intermediate calculations of section 1.2. For the purpose of verifying the correct implementation of the equations, the tables display many more digits than are warranted by the accuracy of the WMM.

The output in Table 3c includes grivation calculations for four grid systems, whether or not the grid system is commonly used in that part of the world. This is helpful for the purposes of verifying correct implementation of the mathematics in the software, and if not used the unwanted grid systems may be ignored.

Table 3a: High-precision numerical example, given values for time, altitude, latitude and longitude.

Time	2022.5000 0000	yr
Height-above-Ellipsoid	100.0000 0000	km
Latitude	-80.0000 0000	deg
Longitude	240.0000 0000	deg

Table 3b: High-precision numerical example, computations of the magnetic field elements

1	lambda	4.18879 02048	rad
2	phi	-1.39626 34016	rad
3	h	1 00000.00000 00000	m
4	t	2022.50000 00000	yr
5	phi-prime	-1.39512 89589	rad
6	r	64 57402.34844 73705	m
7	g(1,0,t)	-29387.75000 00000	nT
8	g(1,1,t)	-1431.45000 00000	nT
9	g(2,0,t)	-2528.75000 00000	nT
10	g(2,1,t)	2964.25000 00000	nT
11	g(2,2,t)	1671.30000 00000	nT
12	h(1,0,t)	0.00000 00000	nT
13	h(1,1,t)	4590.15000 00000	nT
14	h(2,0,t)	0.00000 00000	nT
15	h(2,1,t)	-3067.10000 00000	nT
16	h(2,2,t)	-794.55000 00000	nT
17	Xprime	5758.51760 8019	nT
18	Yprime	14802.96638 39328	nT
19	Zprime	-49761.87672 16040	nT
20	Xprime-dot	28.13532 15304	nT/yr
21	Yprime-dot	1.39706 24624	nT/yr
22	Zprime-dot	85.59909 04809	nT/yr
23	X	5814.96588 86215	nT
24	Y	14802.96638 39328	nT
25	Z	-49755.31199 39183	nT
26	Xdot	28.03819 61827	nT/yr
27	Ydot	1.39706 24624	nT/yr
28	Zdot	85.63095 33031	nT/yr
29	F	52235.35884 49608	nT
30	H	15904.13914 83373	nT
31	D	1.19649 11054	rad
32	I	-1.26141 35720	rad
33	Fdot	-78.04814 71753	nT/yr
34	Hdot	11.55182 44235	nT/yr
35	Ddot	-0.00160 87687	rad/yr
36	Idot	0.00070 97775	rad/yr

Table 3c: High-precision numerical example, grivation calculations. Angles are in degrees.

Grid System	UPS	UPS	UTM	UTM
Grid zone	North	South	10	11
TrueN-to-GridN	240.00000 00000	-240.00000 00000	-2.95450 46801	2.95450 46801
GridN-to-MagN	-171.44610 94350	308.55389 05650	71.50839 52451	65.59938 58849
TrueN-to-MagN	68.55389 05650	68.55389 05650	68.55389 05650	68.55389 05650

1.6 MAGNETIC POLES AND GEOMAGNETIC COORDINATE SYSTEMS

There are different ways of defining magnetic poles. The most common understanding is that they are the positions on the Earth's surface where the geomagnetic field is perpendicular to the ellipsoid, that is, vertical (assuming the deflection of the vertical is negligible). These positions are called *dip poles*, and the north and south dip poles do not have to be (and are not now) antipodal. In principle the dip poles can be found by experiment, conducting a magnetic survey to determine where the field is vertical (Newitt et al., 2009). In practice the geomagnetic field is vertical on oval-shaped loci traced on a daily basis, with considerable variation from one day to the next.

Other magnetic pole definitions originate from models of the geomagnetic field (Table 4). The WMM representation of the field includes a magnetic dipole at the center of the Earth. This dipole defines an axis that intersects the Earth's surface at two antipodal points. These points are called *geomagnetic poles*. The geomagnetic poles, otherwise known as the dipole poles, can be computed from the first three Gauss coefficients of the WMM. Based on the WMM2020 coefficients for 2020.0 the geomagnetic north pole is at 72.68°W longitude and 80.59°N geocentric latitude (80.65°N geodetic latitude), and the geomagnetic south pole is at 107.32°E longitude and 80.59°S geocentric latitude (80.65°S geodetic latitude). The axis of the dipole is currently inclined at 9.41° to the Earth's rotation axis. The same dipole is the basis for the simple geomagnetic coordinate system of geomagnetic latitude and longitude (see section 4, Geomagnetic longitude and latitude in Mercator projection). The geomagnetic equator is at geomagnetic latitude 0°.

The WMM can also be used to calculate dip pole positions. These *model dip poles* are computed from all the Gauss coefficients using an iterative method. In 2020.0 the north dip pole computed from WMM2020 is located at longitude 164.04°E and geodetic latitude 86.50°N and the south dip pole at longitude 135.88°E and geodetic latitude 64.07°S. Past, current and future dip pole positions are available at https://www.ngdc.noaa.gov/geomag/GeomagneticPoles.shtml and https://geomag.bgs.ac.uk/education/poles.html. Over the next five years, the WMM2020 predicts a very slow drift of the south dip pole, at about 9 km/year on average, and a faster (yet gradually decelerating) drift of the north dip pole, at about 41 km/year.

Scientists, map makers and polar explorers have an interest in the dip and geomagnetic pole locations. Although geomagnetic pole observations cannot be made to indicate their positions, these poles are arguably of greater significance than the dip poles. Auroral ovals, which are approximately 5° latitude bands where aurorae are likely to be seen, are approximately centered on the geomagnetic poles. They are usually displaced slightly to the night-side of the geomagnetic poles and greatly vary in size: bands of greatest activity occur between 15° and 25° from the geomagnetic poles.

A further concept is that of *eccentric dipole*, or off-centered dipole. The location of the center of the eccentric dipole (sometimes known as magnetic center), computed using the first eight Gauss coefficients for 2020.0 (Langel, 1987, p. 386), is at (r, φ', λ) = (591 kilometers, 22.67°N, 136.97°E). The axis of the eccentric dipole is parallel to the axis of the (centered) dipole field.

Table 4: Computed pole positions based on the WMM2020.

	Date	North	South
Geomagnetic Poles	2020.0	72.68° W 80.59° N (geocentric) 80.37° S (geodetic)	107.32° E 80.59° S (geocentric) 80.37° S (geodetic)
Model Dip Poles	2020.0	164.04° E 86.50° N (geodetic)	135.88° E 64.07° S (geodetic)
Eccentric Dipole	2020.0	r = 591 km; φ' = 22.67°N; λ = 136.97°E	

1.7 BLACKOUT ZONES

In an effort to provide better guidance to navigators and users, a new product has been created for WMM2020 called the “Blackout Zone” (BoZ). BoZs are generated for, both, the north and south magnetic poles. The BoZs provide improved geographic delineation to navigators as to where they can trust their compass. In the Blackout Zone, WMM declination values are not accurate and compasses are not to be trusted. In addition, BoZ Caution Zones surround the BoZs to alert navigators of increasingly unreliable compass accuracy (see Figure 2). Requirements for the BoZs are described in MIL-PRF-89500B (Department of Defense, 2019).

Previously, the United States Department of Defense (DoD) Safety of Navigation (SoN) guidance included the following warning on all polar maps and charts (Defense Mapping Agency, 1981):

> “The compass becomes increasingly unreliable approaching the magnetic pole from a distance of approximately 1000 miles”.

Since the magnetic poles move significantly over time and paper products may not be updated to reflect this information, the warning was stamped on all maps and charts that covered areas within 1000 miles of the geographic poles (see Figure 2). With the prevalence of easily updatable digital maps, DoD has taken steps to provide the new BoZs for polar SoN.

Compass needles align with the horizontal magnetic field lines allowing users to see where magnetic north is from their current location. Over most of the globe, the magnetic field lines are near parallel to the Earth’s surface. However, at the magnetic poles the magnetic field lines are vertical, which is why a compass will not work well. The needle in the compass will want to point vertically and the result is a spinning needle. The BoZs are calculated to cover regions of the Earth where the horizontal component of the magnetic field is significantly weaker than the vertical component of the magnetic field.

Specifically, the BoZs are defined as constantly moving regions of the WGS 84 ellipsoid where the horizontal intensity (H) is less than 2000 nT. Each BoZ is surrounded by a Caution Zone where the horizontal intensity is less than 6000 nT. The BoZ regions are provided to users in the form of shapefiles available at ftp://ftp.ngdc.noaa.gov/geomag/wmm/wmm2020/shapefiles/, and are plotted on some maps for visualization purposes (see section 1.10). In addition, both NGA

products and the online calculators provided by NCEI include warnings to navigators approaching the BoZs.

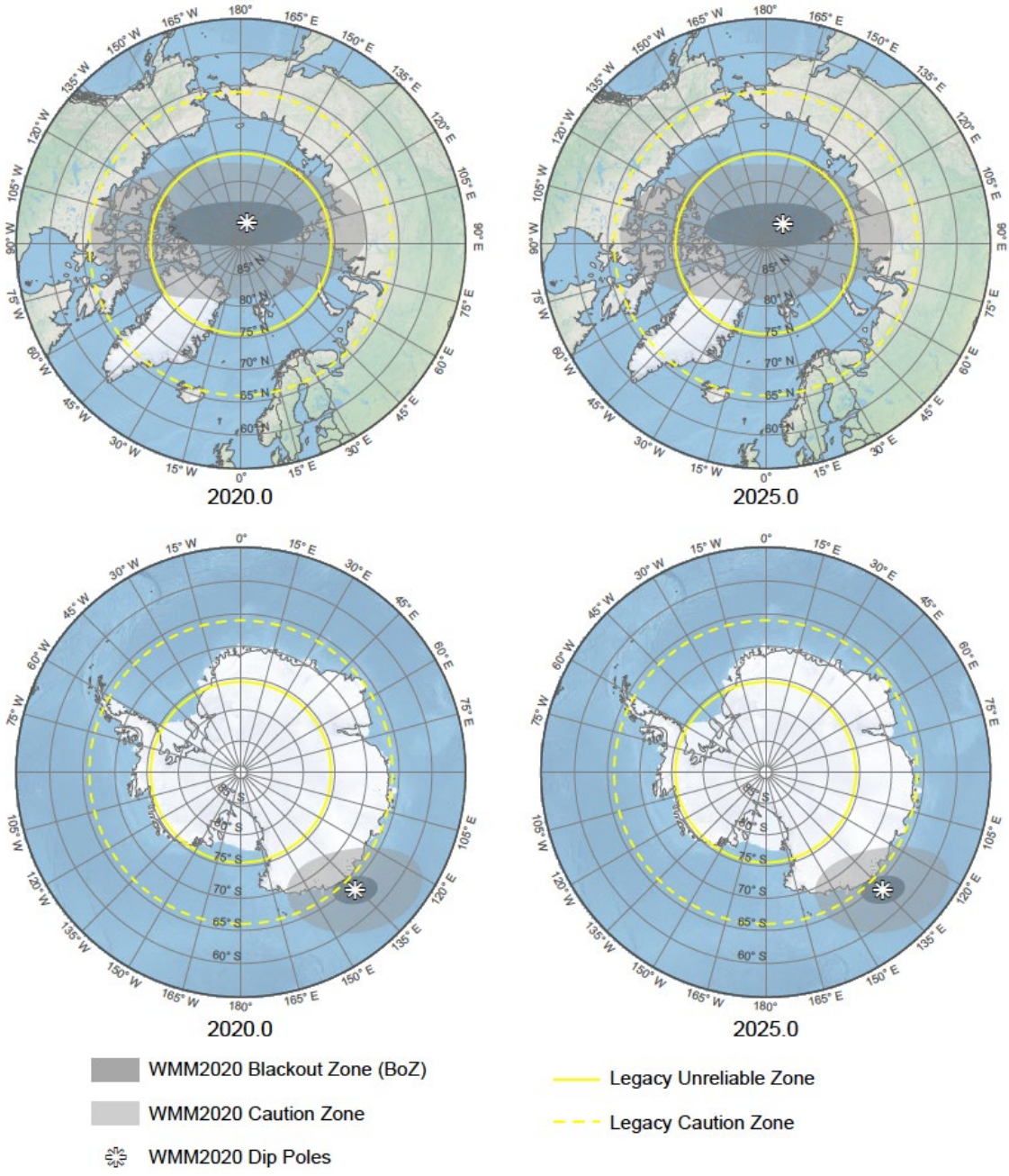

Figure 2: BoZ refinement against legacy warning zones. BoZ and Caution Zone shown at epoch 2020.0 in the Northern (top) and Southern (bottom) Hemispheres.

NCEI Warnings: "Warning: location is in the blackout zone around the magnetic pole as defined by the WMM military specification (https://www.ngdc.noaa.gov/geomag/WMM/data/MIL-PRF-89500B.pdf). Compass accuracy is highly degraded in this region." [triggered if $H < 2000$ nT]

"Caution: location is approaching the blackout zone around the magnetic pole as defined by the WMM military specification (https://www.ngdc.noaa.gov/geomag/WMM/data/MIL-PRF-89500B.pdf). Compass accuracy may be degraded in this region." [triggered if $H \geq 2000$ nT and $H < 6000$ nT]

NGA Warning: "This location is, either approaching or within the magnetic blackout zone defined by the World Magnetic Model (WMM) military specification, MIL-PRF-89500B. Compass accuracy is increasingly unreliable approaching the blackout zone where declination errors exceed 1 degree; and highly degraded within the blackout zone where declination errors of up to 180 degrees will occur. The large declination errors are a result of weak horizontal magnetic intensity and proximity of the magnetic pole."

There are two important facts to note regarding the new BoZs that must be understood before implementation in navigation systems. First, the BoZs will move over time with the magnetic poles. WMM2020 provides the location of the BoZs until December 2024 and it will be the user's responsibility to utilize the correct BoZ for the current time.

The second important fact to note is that the BoZs denote regions where compass reliability gets increasingly worse, not hard limits on where a compass cannot be used. In other words, the compass will not work perfectly 1 meter outside the BoZ and fail 1 meter within. The Caution Zone provides a buffer to assist navigators in this regard.

Figure 2 and Table 5 show the refinement of the BoZs compared against legacy paper map guidance. For the Arctic Region, the area of unreliability is reduced by over 6 million square kilometers and the area of caution is reduced by over 14 million square kilometers. The Antarctic Region reduces the area of unreliability and area of caution significantly more, and more appropriately portrays the warning zone near the magnetic pole not the geographic pole.

Table 5: BoZ size reduction against legacy warning zones. All surface areas in square kilometers on the WGS 84 ellipsoid. WMM2020 values calculated at epoch 2020.0.

	Arctic	Antarctic
Legacy Unreliable Zone	8,093,922	8,093,922
WMM2020 BoZ (Unreliable Zone)	1,546,593	279,633
Difference	6,547,329	7,814,289
Legacy Caution Zone	22,221,903	22,221,903
WMM2020 Caution Zone	7,912,969	2,311,451
Difference	14,308,934	19,910,452

1.8 SUPERSESSION OF THE MODELS

WMM2020 supersedes WMM2015 (Chulliat et al., 2015) and WMM2015v2 (Chulliat et al., 2019) and should replace them in navigation and other systems. Also included with the model is software for computing the magnetic field components *X, Y, Z, H, F, I, D* and auxiliary angles GV_N and GV_S as defined above, as well as the blackout zone products and the model uncertainty on each component (see section 3). WMM2020 is to be used from 1 January 2020, to 31 December 2024. In December of 2024, barring unforeseen circumstances, the U.S. and U.K. agencies will replace WMM2020 with a new degree and order 12 main field model, and a new degree and order 12 predictive secular-variation model.

1.9 POLICY ON ALTERNATE SOFTWARE FOR THE U.S. DEPARTMENT OF DEFENSE

The WMM2020 product release includes several software items by which the WMM2020 model may be computed and/or its subroutines incorporated into larger U.S. Department of Defense (DoD) systems. It is hoped that the software provided is useful for most occasions of DoD systems procurement and development.

If there are special requirements, and the model equations must be implemented anew or a separate interpolation algorithm invented, the software developer may use the label WMM2020 for the resulting product provided the resulting software agrees with the relevant model equations within the following tolerances:

Between latitudes 89.992°S and 89.992°N,

Quantities in nanotesla (nT) shall be correct to within 0.1 nT

Quantities in nanotesla (nT) per year shall be correct to within 0.1 nT/year

(see section 1.4 for the computation problems exactly at the Poles).

This policy is designed to promote interoperability and to track departures from consistency when necessary. It permits systems developers to display as many digits as needed and not display unneeded digits. It also allows that the computations be taken to less than full double precision accuracy and the software retain the WMM2020 label. This policy refers to the allowed computational error in the software, not to the accuracy or limitations of the science or the geomagnetic model.

If there are special requirements, and the model equations are implemented anew or separate interpolation algorithm invented, and accuracy is sacrificed for speed of computation such that the above tolerances are not met, the label WMM2020 may not be applied to the resulting product. In this situation, the DoD entity or contractor is urged to apply to NGA or NCEI acting on behalf of NGA, for the label to adopt to indicate that this is a modification of WMM2020.

1.10 DESCRIPTION OF CHARTS

Charts of magnetic elements and their annual rates of change, and of grid variation, are available from the NOAA WMM web site (https://www.ngdc.noaa.gov/geomag/WMM/image.shtml). Some charts are replicated in section 4. They are also available at the BGS WMM web site (http://www.geomag.bgs.ac.uk/research/modelling/WorldMagneticModel.html).

The following charts are available:

- Main field magnetic elements *X, Y, Z, H, F, I* and *D* on the Miller projection between geodetic latitudes 90°S and 90°N.
- Main field magnetic elements *X, Y, Z, H, F, I* and *D* on the north and south polar stereographic projection for geodetic latitudes northward of 55°N and southward of 55°S.
- Secular variation of *X, Y, Z, H, F, I* and *D* on the Miller projection between geodetic latitudes 90°S and 90°N.
- Secular variation of *X, Y, Z, H, F, I* and *D* on the north and south polar stereographic projection for geodetic latitudes northward of 55°N and southward of 55°S.
- Grid variation (GV) on the north and south polar stereographic projection for geodetic latitudes northward of 55°N and southward of 55°S.
- Geomagnetic latitude and longitude on the Miller projection between geodetic latitudes 90°S and 90°N.

Each chart comes in two versions: with blackout zone and without.

1.11 SOFTWARE, ONLINE CALCULATORS AND TEST VALUES

The WMM coefficient file, software that computes WMM values, and several derived products are distributed by NOAA/NCEI and BGS both online and offline on behalf of NGA and DGC. They are available from https://www.ngdc.noaa.gov/geomag/WMM/soft.shtml.

WMM online calculators allow users to compute values of the magnetic field at any point within the spatial domain of validity of the model, and at any time between the model release and 2025.0. Various input and output formats are available, as well as web-based application programming interfaces (API). The calculators are available at

- https://www.ngdc.noaa.gov/geomag/WMM/calculators.shtml
- https://geomag.bgs.ac.uk/data_service/models_compass/wmm_calc.html

To verify the correctness of a coefficient update or new software installation, Table 6 provides test values to validate software output.

Table 6: WMM2020 test values. The computation was carried out with double precision arithmetic. Single precision arithmetic can cause differences of up to 0.1 nT. Heights are with respect to the WGS 84 Ellipsoid. Grid Variation is with respect to the Grid North of the Universal Polar Stereographic Projection.

Date	Height (km)	Lat (deg)	Lon (deg)	X (nT)	Y (nT)	Z (nT)	H (nT)	F (nT)	I (deg)	D (deg)	GV (deg)
2020.0	0	80	0	6570.4	-146.3	54606.0	6572.0	55000.1	83.14	-1.28	-1.28
2020.0	0	0	120	39624.3	109.9	-10932.5	39624.4	41104.9	-15.42	0.16	
2020.0	0	-80	240	5940.6	15772.1	-52480.8	16853.8	55120.6	-72.20	69.36	-50.64
2020.0	100	80	0	6261.8	-185.5	52429.1	6264.5	52802.0	83.19	-1.70	-1.70
2020.0	100	0	120	37636.7	104.9	-10474.8	37636.9	39067.3	-15.55	0.16	
2020.0	100	-80	240	5744.9	14799.5	-49969.4	15875.4	52430.6	-72.37	68.78	-51.22
2022.5	0	80	0	6529.9	1.1	54713.4	6529.9	55101.7	83.19	0.01	0.01
2022.5	0	0	120	39684.7	-42.2	-10809.5	39684.7	41130.5	-15.24	-0.06	
2022.5	0	-80	240	6016.5	15776.7	-52251.6	16885.0	54912.1	-72.09	69.13	-50.87
2022.5	100	80	0	6224.0	-44.5	52527.0	6224.2	52894.5	83.24	-0.41	-0.41
2022.5	100	0	120	37694.0	-35.3	-10362.0	37694.1	39092.4	-15.37	-0.05	
2022.5	100	-80	240	5815.0	14803.0	-49755.3	15904.1	52235.4	-72.27	68.55	-51.47
Date	**Height (km)**	**Lat (deg)**	**Lon (deg)**	**Xdot (nT/yr)**	**Ydot (nT/yr)**	**Zdot (nT/yr)**	**Hdot (nT/yr)**	**Fdot (nT/yr)**	**Idot (deg/yr)**	**Ddot (deg/yr)**	
2020.0	0	80	0	-16.2	59.0	42.9	-17.5	40.5	0.02	0.51	
2020.0	0	0	120	24.2	-60.8	49.2	24.0	10.1	0.08	-0.09	
2020.0	0	-80	240	30.4	1.8	91.7	12.4	-83.5	0.04	-0.10	
2020.0	100	80	0	-15.1	56.4	39.2	-16.8	36.9	0.02	0.51	
2020.0	100	0	120	22.9	-56.1	45.1	22.8	9.8	0.07	-0.09	
2020.0	100	-80	240	28.0	1.4	85.6	11.4	-78.1	0.04	-0.09	
2022.5	0	80	0	-16.2	59.0	42.9	-16.2	40.7	0.02	0.52	
2022.5	0	0	120	24.2	-60.8	49.2	24.2	10.5	0.08	-0.09	
2022.5	0	-80	240	30.4	1.8	91.7	12.6	-83.4	0.04	-0.09	
2022.5	100	80	0	-15.1	56.4	39.2	-15.5	37.1	0.02	0.52	
2022.5	100	0	120	22.9	-56.1	45.1	23.0	10.2	0.07	-0.09	
2022.5	100	-80	240	28.0	1.4	85.6	11.6	-78.0	0.04	-0.09	